Histol Histopathol (2023) 38: 113-126

http://www.hh.um.es

Histology and Histopathology
From Cell Biology to Tissue Engineering

ORIGINAL ARTICLE **Open Access**

Long non-coding RNA XIST promotes the malignant features of oral squamous cell carcinoma (OSCC) cells through regulating miR-133a-5p/VEGFB

Kankui Wu[1]*, Wancui Wu[1]*, Mengxuan Wu[2,3] and Wenzhe Liu[1]

[1]Department of Stomatology, the Second Affiliated Hospital of Guangzhou Medical University,

[2]Department of Stomatology, the First Affiliated Hospital of Jinan University and [3]School of Stomatology, Jinan University, China

*Kankui Wu and Wancui Wu contributed equally to this work

Summary. Objective. Oral squamous cell carcinoma (OSCC) represents a frequently seen oral cavity malignancy, and the mechanisms of its occurrence and development remain unclear. The present work examined the expression and biological function of long non-coding RNA (lncNRA) XIST (X-inactive specific transcript) in OSCC cells and tissues.

Study design. A total number of 50 OSCC and paired non-carcinoma tissue samples were collected in this study. Gene expression levels in cancer tissues and cells were quantified by RT-qPCR. In addition, gain- and loss-of-function experiments were conducted to investigate the biological roles of XIST as well as its downstream targets in OSCC cells.

Results. XIST was upregulated in OSCC cells and tissues, which predicted a poorer prognostic outcome in OSCC patients. Silencing XIST inhibited the growth and invasion of OSCC cells and triggered apoptosis. miR-133a-5p was identified as a downstream target of XIST, which was downregulated in OSCC tissues. miR-133a-5p mediated the effect of XIST by targeting VEGFB. VEGFB overexpression rescued the inhibitory effects of XIST silencing on cell growth, invasion and migration.

Conclusion. Taken together, the above data indicates that XIST serves as an oncogenic factor to enhance the growth and invasion of OSCC cells by targeting the miR-133a/VEGFB axis.

Key words: XIST, Long non-coding RNA, OC, miR-133a-5p, VEGFB

Corresponding Author: Wenzhe Liu, 250, East Changgang Road, Haizhu District, 510260, Guangzhou, Guangdong Province, China. e-mail: qerk211@163.com

DOI: 10.14670/HH-18-504

Introduction

Oral cancer (OC) is a malignant tumor frequently found in tongue, floor of mouth and the lining of lip within the oral cavity boundaries, among which, oral squamous cell carcinoma (OSCC) is a prevalent subtype (Petti et al., 2013). With an approximately annual case of 354,864 globally, OC has become a common cancer which accounts for 177,384 deaths yearly (Petti et al., 2013; Bray et al., 2018). Sri Lanka, India, Pakistan, Bangladesh, Hungary, and France are among the countries with the highest rate of oral cancer (Ferlay et al., 2010). The causative agents for oral cancer are multifactorial: except for multiple genetic and epigenetic factors, drinking and smoking are recognized as two primary risk factors for oral cancer development (Blot et al., 1988; Figuero Ruiz et al., 2004). The survival rate of OSCC patients at 5 years has not increased in the last few years despite the implementation of clinical therapeutic modalities like chemotherapy, surgery and radiotherapy (Petti et al., 2013; Bray et al., 2018). The investigation of molecular mechanisms underlying OSCC progression may provide insights into therapeutic intervention to improve the treatment outcome.

As the next-generation sequencing (NGS) technique has been widely applied, an increasing number of non-coding RNAs (ncRNAs) has been discovered in the human genome (Esteller, 2011). Long ncRNAs (lncRNAs) are ncRNAs over 200 nucleotides in length (Mercer et al., 2009). LncRNAs are implicated in a myriad of biological events in carcinogenesis by regulating RNA splicing, chromatin structure, and gene expression via targeting microRNAs (miRNAs) (Kondo et al., 2017). The aberrant expression of lncRNAs in tumor cells can lead to drug resistance and augmented aggressiveness through different regulatory mechanisms and signaling pathways (Xia and Hui, 2014). X-chromosome inactive specific transcript (XIST), a master modulator in female mammals during early

development, has been extensively investigated (Cerase et al., 2015). As reported in recent works, XIST plays crucial roles in carcinogenesis of diverse malignant tumors, including lung cancer, pancreatic cancer, colorectal cancer (CRC), cervical cancer (CC), bladder, gastric cancer (GC) and papillary thyroid cancer (PTC), through modulating epithelial-mesenchymal transition (EMT), cell growth and migration (Zhou et al., 2013; Hu et al., 2017, 2019; Ma et al., 2017; Lv et al., 2018; Sun et al., 2018; Zhu et al., 2018; Liu et al., 2019a; Zhang et al., 2019). Interestingly, lncRNAs frequently interact with miRNAs to regulate tumor biology. miRNAs represent the single-stranded ncRNAs that are 19-25 nucleotides in length. One of the well-established roles of miRNAs is to target the complementary sequences on mRNA, leading to inhibition of mRNA translation or mRNA degradation (Vennin et al., 2015). miRNA expression profiles vary among different cancers and the dysregulation of certain miRNAs seems to be of great value in the diagnosis and prediction of therapy response (Esteller, 2011). Among them, miR-133a has been reported to be downregulated in multiple malignant tumors, such as bladder, gastric, lung and prostate cancer (Tao et al., 2012; Zhou et al., 2013; Cheng et al., 2014; Liu et al., 2019b; Wang et al., 2019; Yin et al., 2020; Zheng et al., 2020b; Guo et al., 2021). However, miR-133a expression pattern in OSCC and its potential roles need to be investigated. Besides, whether miR 133a mediates the effect of XIST in OSCC needs to be clarified.

Vascular endothelial growth factors (VEGFs) belong to the VEGF/PDGF (platelet-derived growth factor) hormone family, with highly conserved receptor-binding structure (Vitt et al., 2001). VEGFB is a key VEGF family member with a critical function in development, gene expression control, as well as functional differentiation of adipocytes (Jin et al., 2018). It was reported that the reduced expression of VEGFB in diabetic heart is associated with an enhanced cell death signal transduction (Lal et al., 2017). VEGFB and its receptor are implicated in different pathological progressions, including malignant carcinogenesis (Kim et al., 2015; Jin et al., 2018). As demonstrated in a previous study, increased VEGF expression supports angiogenesis and progression in OSCC (Kim et al., 2015). However, the mechanisms underlying VEGF dysregulation remain unclear.

In the present work, the expression pattern and functional role of lncRNA XIST have been investigated in OSCC cells. XIST expression was examined in 50 pairs of OSCC and matched non-carcinoma tissue samples, and compared between OSCC cells and normal oral keratinocytes. Loss- and gain-of-function experiments were conducted to study the biological roles of XIST in supporting the malignant phenotype of OSCC cells. XIST was upregulated in OSCC cells and tissues, and silencing XIST inhibited the growth and invasion of OSCC cells. miR-133a-5p was identified as a downstream target of XIST, which mediated the effect of XIST by targeting VEGFB. Collectively, this study indicates that XIST serves as an oncogenic factor to promote the growth and invasion of OSCC cells by targeting miR-133a/VEGFB axis.

Materials and methods

Human samples

OSCC tumor samples and matched non-carcinoma tissues (para-cancerous tissues) were collected in patients (n=50) diagnosed with OSCC at the Second Affiliated Hospital of Guangzhou Medical University between 1 Jan, 2017 and 31 Aug, 2018. All the cases enrolled in the study had not gone through radiotherapy and chemotherapy prior to sample collection. Table 1 summarizes clinical characteristics based on the expression level of XIST. The primary lesions for the tumor collection were from oral floors or tongues. All the samples were surgically resected, followed by snap-freezing under -80°C conditions for further experiments. All patients signed the informed consent. The Ethics Committee of Second Affiliated Hospital of Guangzhou Medical University approved our study protocols (2018615).

Cell culture

Normal human oral keratinocytes (NHOK) and OSCC cells (HSC-2, SCC9, SAS, CAL-27) were purchased from American Type Culture Collection

Table 1. Correlation between XIST expression and the clinical features.

Variable	Number	XIST expression	
		Low	High
Age (years)			
< 60	16	9	7
≥ 60	34	16	18
Gender			
Male	29	14	15
Female	21	11	10
Smoking			
Non-smoker	13	7	6
Smoker	37	18	19
Primary lesions			
Oral floor	22	13	9
Tongue	28	13	15
Tum size (cm)			
< 3	26	15	11
≥ 3	24	10	14
TNM staging			
I-II	20	12	8
III-IV	30	13	17
Lymph node metastasis			
No	28	13	15
Yes	22	12	10

(Manassas, VA, USA). The origins of OSCC cell lines: HSC-2 (Oral cavity floor), SCC9 (Tongue), SAS (Tongue), CAL-27 (Tongue). Cells were cultured in high-glucose (HG) DMEM that included 10% fetal bovine serum (FBS) (Thermo Fisher Scientific, Waltham, MA, USA) along with 1% penicillin/streptomycin (Corning, Glendale, NY, USA), and 2 mM glutamine (Corning, Glendale, NY, USA), and maintained under 37°C and 5% CO_2 conditions in a humid incubator.

RNA isolation and quantitative real-time PCR (qRT-PCR)

Trizol reagent (Thermo Fisher Scientific, Waltham, MA, USA) was used to isolate total RNA from tissues and cells according to the manufacturer's instructions. Thereafter, cDNA was synthesized using purified total RNA (1 μg) with the iScript cDNA synthesis kit (Bio-Rad, Hercules, CA, USA). qPCR analysis was conducted to quantify cDNA with SYBR-Green supermix (Bio-Rad, Hercules, CA, USA) on the Cycler Thermal Cycler (Bio-Rad, Hercules, CA, USA). The conditions for PCR procedure were as follows, 5 min at 95°C; 30 s at 95°C, 30 s at 60°C as well as 60 s at 72°C for 40 cycles, and signals were detected after every cycle. $2^{-\Delta\Delta Ct}$ approach was employed to analyze the relative gene expression, with GAPDH as the endogenous control of coding gene (VEGFB), with U6 being the internal control of non-coding RNAs (XIST and miR-133a-5p). The primers utilized in the present work are shown in Table 2.

Cell transfection

For VEGFB overexpression, VEGFB cDNA was cloned in the pcDNA3.1 vector (RiboBio, Guangzhou, China), with empty pcDNA3.1 vector as the negative control (NC). miR-133a-5p mimic, siRNA XIST1 together with the miR-NC (negative control for miRNA) was prepared by GenePharma (Shanghai, China). siRNA sequences were listed as below:
siRNA for XIST #1 (si-XIST #1):
5'-UGGAUUUGUACCAUUCUUCUG-3';
siRNA for XIST #2 (si-XIST #2):
5'-ACUCAUUGGUUCCUUUAAGGG-3";
si-NC (NC of siRNA):
5'-CCCAGUUACGAATCGCUUCCA-3'.

Transfection or co-transfection of cells was carried out using Lipofectamine 2000 (Invitrogen, Waltham, MA, USA) following specific instructions. 4 μg plasmid and miR-133a-5p mimic, siRNA or the NC (100 nM) were used to transfect cells in 6 well plate with 80% confluency. At 48 h post-transfection, transfected cells were harvested to carry out subsequent analyses.

Cell proliferation experiment

HSC-2 and SCC9 cells showing the highest level of XIST expression were selected to perform functional experiments. Cell viability was measured using Cell Counting Kit-8 (CCK-8) assay (Solarbio, Beijing, China). 48 hours after transfection, OSCC cells (1500/well) were seeded in 96-well plates with three replicates, followed by incubation for indicated durations. CCK-8 solution (10 μL) was added to each well at indicated time points, followed by another 2h incubation under 37°C. Finally, the spectrophotometer (Bio-Rad, Hercules, CA, USA) was utilized to measure the absorbance (OD) value at 450 nm.

Clone forming assay

HSC-2 and SCC9 cells showing the greatest XIST levels were selected for colony formation assay. After specific treatment, cells were subject to trypsinization and r suspension in the medium. Cells were seeded (1000/well) in the 6-well plates to culture for a 14-day period, and the medium was replenished every 3 days. On the 14 day, 4% paraformaldehyde (PFA) was utilized to fix cells for 10 min at ambient temperature, followed by staining with 0.5% crystal violet (Beyotime, Shanghai, China) for 20 min. Stained cells were imaged and the colonies were counted under Leica AM6000 microscope (Leica, Wetzlar, Germany).

Dual-luciferase reporter assay

The potential miRNA targets of lncRNA XIST were predicted by DINAN tools (http://carolina.imis.athena-innovation.gr/diana_tools/web/index.php). Among the top-ranked hits, miR-133a-5p has been reported to be downregulated in several cancers (Tao et al., 2012; Zhou et al., 2013; Cheng et al., 2014; Liu et al., 2019b; Wang et al., 2019; Yin et al., 2020; Zheng et al., 2020b; Guo et al., 2021), and it was selected as the candidate for detailed investigation. GenePharma (Shanghai, China) was responsible for constructing all the luciferase reporter vectors. To demonstrate the functional interactions, the sequence containing the wild type binding site (WT sequence in XIST or 3' UTR of VEGFB mRNA) cloned into to pmiRGLO luciferase vector (Promega, Madison, WI, USA) to generate WT

Table 2. The list of primer sequences.

Primer	Sequence (5' to 3')	Amplification efficiency
VEGFB_F	TGACATCACCCATCCCACTCC	93.3%
VEGFB_R	GGGCAGGCAGTCTGTATTGA	
GAPDH_F	ACACCCACTCCTCCACCTTT	97.1%
GAPDH_R	TTACTCCTTGGAGGCCATGT	
XIST_F	CCCAGGGAGAGTATGGAGTGA	102.7%
XIST_R	ACCAAGTTCCTCACTGGCTT	
miR-133a-5p_F	TTTGGTCCCCTTCAACC	97.6%
miR-133a-5p_R	GAGCAGGGTCCGAGGT	
U6_F	GCTTCGGCAGCACATATACTAAAA	98.3%
U6_R	CGCTTCACGAATTTGCGTGTCAT	

reporters for XIST and VEGFB. The sequences with mutated binding sites (MUT sequence in XIST or 3' UTR of VEGFB mRNA) were cloned into the luciferase vector to generate MUT reporters for XIST and VEGFB. The reporter plasmid and renilla luciferase (hRlucneo) control plasmid were co-transfected into OSCC cells with either miRNA mimic or miR-NC in a 12-well plate (1×10^5 cells/well) using Lipofectamine 2000 reagent in line with specific instructions. 48h post transfection, dual-luciferase reporter assay kit (Promega, Madison, WI, USA) was used to measure the relative luciferase activities using a luminometer (Tecan, Theale, UK). The reading of firefly luciferase activity in the reporter was normalized to the activity of renilla luciferase in the control vector.

Cell migration and invasion assay

HSC-2 and SCC9 cells showing the highest level of XIST expression were selected for invasion and migration assays. Matrigel-free Transwell chamber (Corning, Glendale, NY, USA) was used for migration assay, whereas Matrigel-coated (BD Biosciences, Bedford, MA, USA) top Transwell chamber was used for cell invasion experiment. $2x10^5$ HSC-2 and SCC9 cells were inoculated in the top Transwell chamber in serum-free medium, and medium with 10% serum (500 μL) was added into the lower chamber. After 24h incubation, 4% PFA was utilized to fix cells migrating to the lower chamber membrane for a 10 min period under ambient temperature. Fixed cells were stained using 0.5% crystal violet (Sigma-Aldrich, St. Lou-is, MO, USA) for a 20 min period. A Leica AM6000 microscope was utilized to image and count the migrating and invading cells on the membrane. Cell numbers from five random fields (400x) in each sample were summarized for quantification.

Western blotting (WB) assay

Transfected HSC-2 and SCC9 cells were suspended in ice-cold RIPA lysis buffer (Cell Signaling Technology, Danvers, MA, USA) for 15 min, and the lysed cells were centrifuged at 14000 rpm for 10 min. The supernatant containing total protein lysate was quantified by a BCA Protein assay kit (Solarbio, Beijing, China). 15 μg of protein sample was separated through SDS-PAGE, followed by transfer onto PVDF membrane using Trans-Blot Turbo™ System (Bio-Rad, Hercules, CA, USA). The membrane was blocked in 5% skim milk for a 1-h period and then incubated overnight with primary antibodies at 4°C: VEGFB, E-cadherin, N-Cadherin, Vimentin and anti-GAPDH antibodies (Santa Cruz Biotech, Dallas, TX, USA, 1:1000 dilutions). After rinsing by TBST 3 times (5 min each), the membrane was further incubated with HRP-labeled secondary antibody (1:3000 dilution; Cell signaling Technologies, Danvers, MA, USA) for 1h at room temperature. After rinsing with TBST, the Amersham ECL Prime chemiluminescence detection kit (GE Healthcare, Chicago, IL, USA) was utilized to visualize protein bands, and Image Quant LAS4000 system (GE Healthcare, Chicago, IL, USA) was employed for photographing and quantitative analysis.

Flow cytometry for apoptosis

Apoptosis was detected by annexin V-FITC Apoptosis Detection Kit (KeyGEN, Jiangsu, China) in line with the manufacturer's protocols. In brief, cells were trypsinized and suspended in 1X Annexin V binding buffer (1000 μL, containing 1 million cells). Then Annexin V-FITC (5 μL) and PI (5 μL) reagents were added to the cell suspension for 30-min incubation in the dark. Cells were rinsed with 1X Annexin V binding buffer, and re-suspended in 400 μL 1X Annexin V binding buffer. The apoptotic events were recorded using LSRII Fortessa Cell Analyzer (BD Biosciences, Franklin Lakes, NJ, USA). FlowJo software (FlowJo LLC, San Carlo, CA, USA) was utilized for flow cytometry data analysis.

Statistics

The *in vitro* assays were conducted in three independent experiments, and the results were expressed as mean ± SD. The association of XIST level with the clinicopathological parameters was evaluated by Chi-square test in Table 1. Unpaired student's t-test was utilized for comparing the significance of differences between 2 groups. One-way ANOVA together with Tukey's post hoc test was adopted for pairwise comparison across multiple groups. Two-way ANOVA was utilized to compare the data across several time points. Kaplan Meier Curve and log-rank test were employed to compare the cumulative survival rates in OSCC patients. Spearman correlation was performed to determine the correlation of the expression levels between two genes. *P<0.05, **P<0.01, ***P<0.001.

Results

LncRNA XIST expression increases in both OSCC cells and tissues, which predicts a dismal prognosis

To investigate the functional roles of XIST in the regulation of OSCC progression, this study examined lncRNA XIST levels in OSCC samples from 50 patients as well as the paired adjacent normal tissues. As revealed by RT-qPCR assay, XIST expression level was significantly upregulated in OSCC samples in comparison with adjacent normal tissues (Fig. 1A). Additionally, XIST levels were also markedly increased in OSCC cell lines (HSC-2, SCC9, SAS, CAL-27) when compared to those in human oral keratinocytes (NHOK) (Fig. 1B). The above results indicate that that the aberrant upregulation of XIST is implicated in the progression of OSCC. Since HSC-2 and SCC9 cells

exhibited the highest XIST expression among the 4 OSCC cell lines, they were selected for the subsequent analysis. Moreover, the association between XIST level and the clinical parameters of OSCC patients were assessed. The median XIST expression level was used as the cutoff to divide the patients into high or low XIST expression group (n=25 each). A high expression of XIST was significantly associated with an advanced TNM tumor stage and greater tumor size (Table 1). However, there were no correlations between age, sex, origin of lesions, and lymph node metastasis with the XIST expression level. Further, the overall survival rate between these two groups was analyzed by Kaplan-Meier curve. Clearly, XIST up-regulation in OSCC patients predicted a poorer overall survival (OS) rate, as well as a poorer progression-free survival (PFS) (Fig. 1C,D). Collectively, based on these results, a high XIST expression suggests a dismal prognosis of OSCC patients, indicating that XIST is a potential prognostic marker for OSCC.

Silencing LncRNA XIST suppresses OSCC cell growth, invasion and migration, and triggers cell apoptosis

To examine the role of XIST in cell migration and invasion, loss-of-function experiments in OSCC cells were performed by silencing XIST using RNA interference. si-NC (Negative control siRNA), si-XIST (siRNA for XIST, si-XIST#1, si-XIST#2) were transfected in HSC-2 and SCC9 cells and the knockdown efficiency was confirmed by RT-qPCR. XIST levels were significantly decreased in cells transfected with si-XIST#1 or si-XIST#2 in comparison with si-NC group (Fig. 2A). si-XIST#1 was selected in the following experiment. According to CCK-8 cell proliferation assay, XIST knockdown remarkably suppressed the cell growth of HSC-2 and SCC9 as compared to si-NC group (Fig. 2B). Colony formation assay further demonstrated that XIST knockdown suppressed the clone forming abilities of HSC-2 and SCC9 cells (Fig. 2C). Meanwhile, after XIST siRNA transfection, HSC-2 and SCC9 cells had significantly impaired invasion and migration (Fig. 2D,E). Furthermore, silencing XIST considerably increased the percentage of apoptotic events in both HSC-2 and SCC9 cells (Fig. 2F). We also examined the protein markers related to EMT by Western blot. The results showed that silencing XIST reduced the expression of N-cadherin and Vimentin, while promoting the expression of E-cadherin (Fig. 2G). These data suggest that silencing XIST impaired the EMT processes in OSCC. In conclusion, the above results suggest the critical function of XIST in promoting cell proliferation, migration, invasion and EMT in OSCC cells.

miR-133a-5p is a target of lncRNA XIST, which is negatively regulated by XIST in OSCC cells

To determine the potential downstream miRNA targets of XIST, an online software DIANA tool was used for miRNA target searching. The analysis revealed that XIST contains miR-133a-5p's potential binding site (Fig. 3A). To validate the functional association of XIST with miR-133a-5p, miR-133a-5p expression was

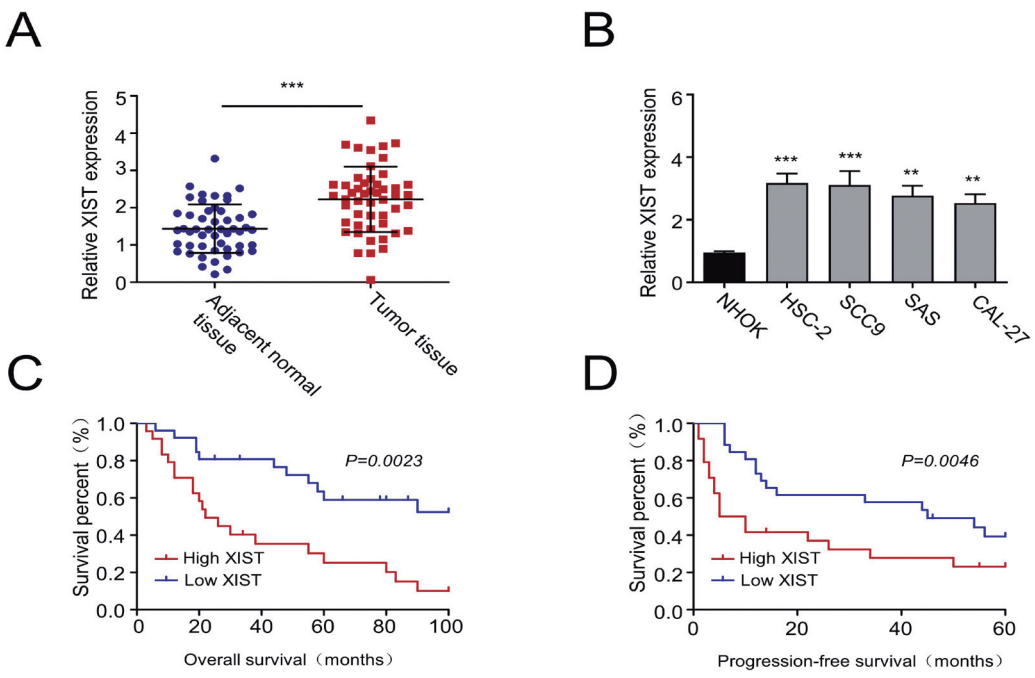

Fig 1. XIST is up-regulated in OSCC cells and tissues. **A.** The relative XIST levels within OSCC and paired non-carcinoma tissue samples (n=50), determined through RT-qPCR. Results were standardized based on GAPDH expression. **B.** XIST expression levels in OSCC cells including HSC-2, SCC9, SAS and CAL-27, together with normal human oral keratinocytes (NHOK) were detected through RT-qPCR. Data were the summary of three independent experiments, which were normalized to GAPDH mRNA. **C.** According to Kaplan-Meier Curve analyses, LncRNA XIST up-regulation predicted the poor OS of OSCC cases. **D.** Elevated XIST level predicts the dismal PFS by Kaplan Meier Curve analysis. *P<0.05, **P<0.01, ***P<0.001.

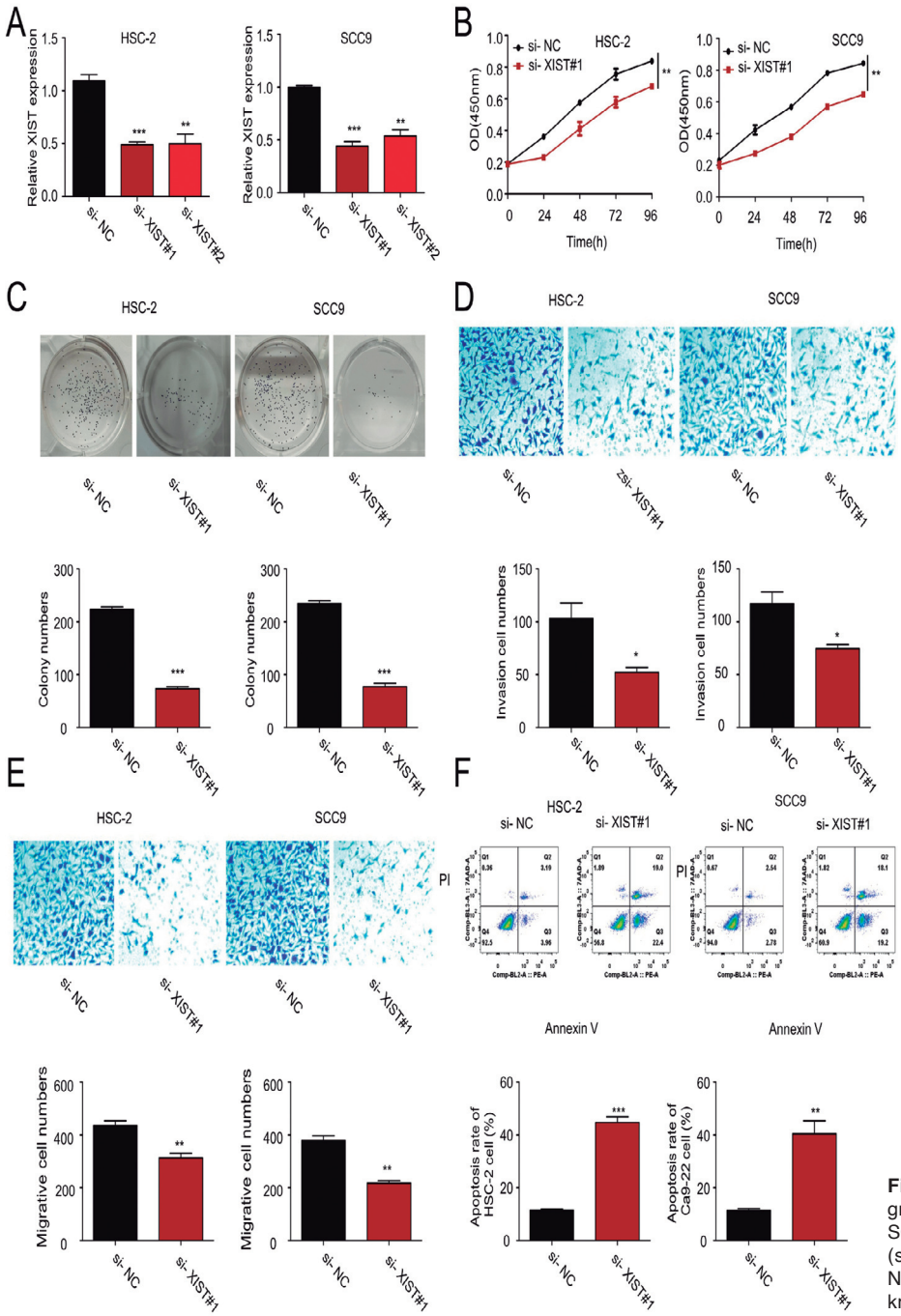

Fig 2. XIST knockdown restrains OSCC cell growth and induces apoptosis. **A.** HSC-2 and SCC9 cells were transfected with XIST siRNA (si-XIST#1, si-XIST#2) or control siRNA (si-NC), RT-qPCR was conducted to analyze XIST knockdown efficiency. We used si-XIST#1 in the following assays. **B.** Growth curves of HSC-2 and SCC9 cells were assessed by CCK-8 assay at diverse times (0/24/48/72/96 h) following si-XIST1# RNA transfection. **C.** Colony formation capacity in XIST-silenced HSC-2 and SCC9 cells was analyzed through clone forming assay. **D-E.** We conducted Transwell assays to determin cell migration ability **(D)** and invasion ability **(E)** after XIST knockdown. **F.** Flow cytometric analysis on apoptotic events in cells with/without XIST knockdown. **G.** Western blot analysis of EMT markers (N-cadherin, Vimentin, E-cadherin) in cells with/without XIST knockdown. Results represent means from 3 individual assays. *P<0.05, **P<0.01, ***P<0.001.

evaluated within HSC-2 and SCC9 cells after XIST silencing. Clearly, miR-133a-5p level was significantly elevated after XIST knockdown (Fig 3B). We further generated luciferase reporter with wild type (WT) or mutated (MUT) binding sites between XIST/miR-133a-5p to confirm the functional association. As revealed by the dual-luciferase reporter assay, miR-133a-5p mimic remarkably suppressed the luciferase activity of WT reporter, whereas the suppression was abrogated in the MUT reporter (Fig. 3C). Furthermore, miR-133a-5p expression was markedly downregulated in OSCC tumor samples (Fig. 3D), and Spearman correlation analysis suggests that XIST expression level was negatively correlated with miR-133a-5p levels in OSCC samples (Fig 3E). Together, the above data suggest that XIST interacts with miR-133a-5p within OSCC cells to negatively regulate its expression.

miR-133a-5p mimic recapitulates the role of XIST silencing in OSCC cell growth and migration

To further examine the dependence of XIST on miR-133a-5p, HSC-2 and SCC9 cells were transfected with miR-NC, miR-133a-5p mimic, miR-133a-5p mimic with si-NC or si-XIST. As revealed by CCK-8 cell proliferation assay, miR-133a-5p mimic transfection suppressed OSCC cell growth, while the co-transfection with si-XIST further inhibited their proliferation (Fig. 4A). Clone forming assay showed similar synergistic effects of miR-133a-5p mimic and si-XIST (Fig. 4B). Furthermore, miR-133a-5p mimic transfection inhibited HSC-2 and SCC9 cell invasion and migration, which was further impaired when si-XIST was co-transfected (Fig. 4C,D). Collectively, miR-133a-5p overexpression can recapitulate the impact of XIST silencing on OSCC cells.

VEGFB serves as a downstream target of miR-133a-5p in OSCC cells

Next, the downstream mRNA targets of miR-133a-5p were predicted using DIANA bioinformatics tool. As a result, VEGFB showed potential binding sites for miR-133a-5p at its 3' UTR (Fig. 5A). As revealed by dual-

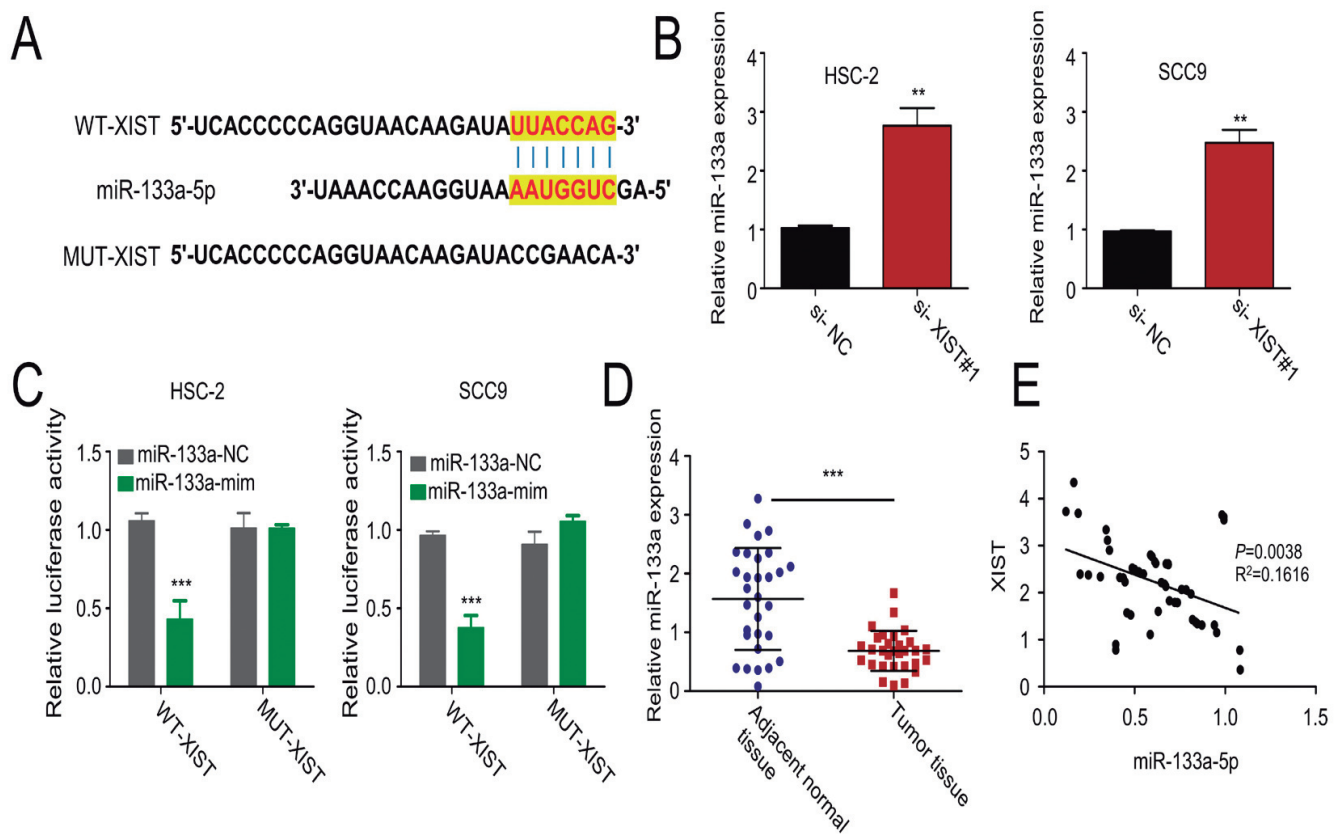

Fig 3. Interaction of lncRNA with miR-133a-5p within OSCC cells. **A.** DINAN online tool was adopted to predict binding sequence of miR-133a-5p with XIST. **B.** miR-133a-5p levels within HSC-2 and SCC9 cells transfected with XIST siRNA were determined through RT-qPCR. **C.** Co-transfection of MUT or WT XIST luciferase reporter construct together with miR-133a-5p mimic or miR-NC into HSC-2 and SCC9 cells. The effects of the miR-133a-5p mimic on XIST reporters (Wild type and mutated reporter) were analyzed via dual-luciferase reporter assay. **D.** miR-133a-5p levels in OSCC tissues were measured through RT-qPCR **E.** Association of XIST expression with miR-133a-5p within OSCC tissue samples determined by Spearman correlation. Data are summary from 3 individual assays. *P<0.05, **P<0.01, ***P<0.001.

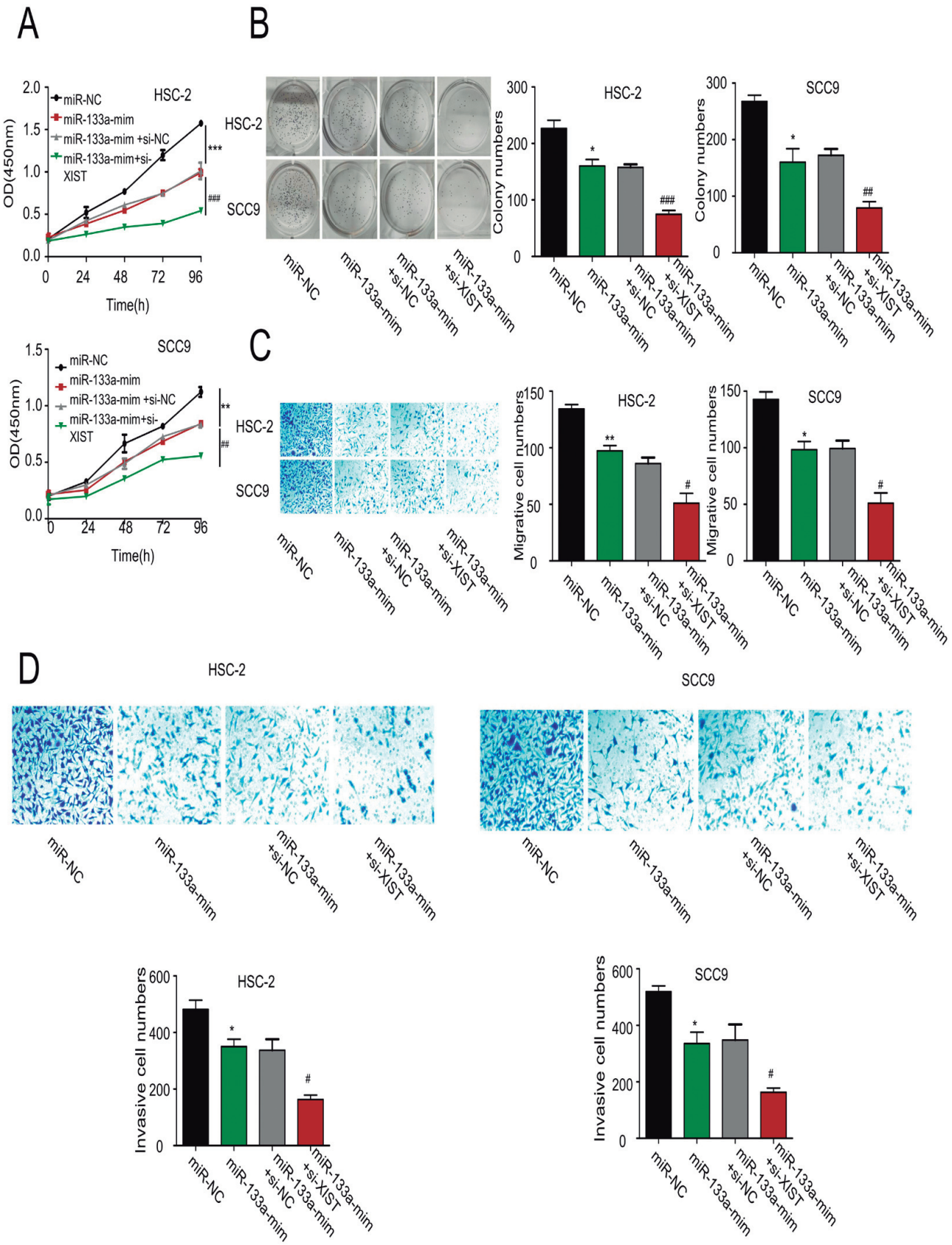

Fig 4. Role of XIST silencing in miR-133a-5p's biological function within OSCC cells. miR-133a-5p mimic, miR-133a-5p mimic + si-XIST (XIST siRNA), miR-NC and miR-133a-5p mimic + si-NC (siRNA negative control) were transfected into HSC-2 and SCC9 cells. **A.** Cell proliferation at 0/24/48/72/96 h post-transfection was measured by CCK-8 assay. **B.** Cell proliferation capacity was measured through clone forming assay. Cell migration **(C)** and cell invasion **(D)** *in vitro* were analyzed via Transwell assay. Results represent the means from 3 individual assays. *P<0.05, **P<0.01, ***P<0.001; # indicates statistical comparison between miR-133a-5p mimic and miR-133a-5p mimic + si-XIST groups.

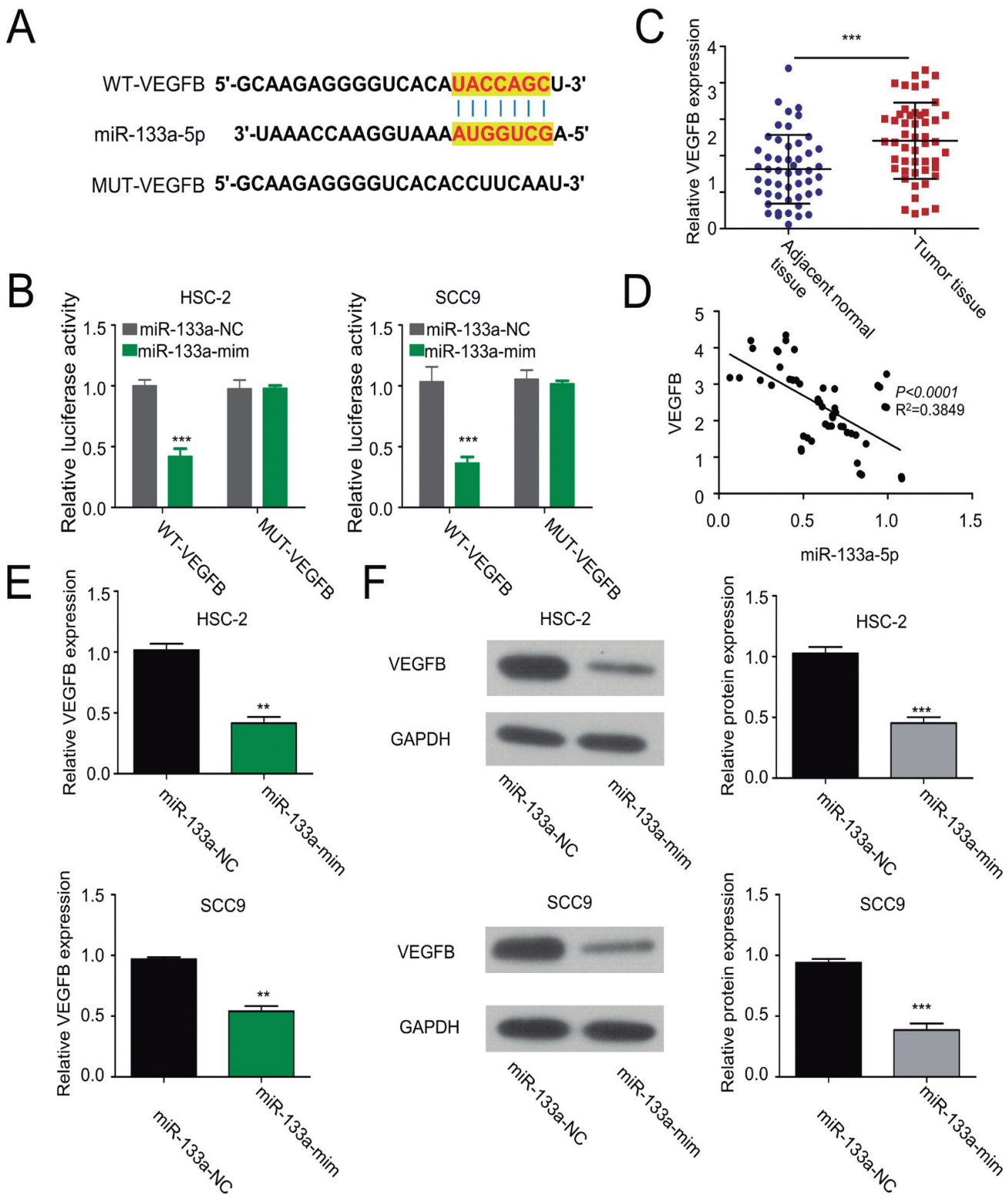

Fig 5. miR-133a-5p modulates VEGFB expression within OSCC cells. **A.** miR-133a-5p's possible binding site was estimated within 3′-UTR in VEGFB mRNA by bioinformatics analysis (DINAN tools). **B.** Co-transfection of MUT and WT VEGFB luciferase reporter construct and miR-133a-5p mimic or miR-NC into HSC-2 and SCC9 cells. The effects of the miR-133a-5p mimic on VEGFB reporters (Wild type and mutated reporter) were analyzed via dual-luciferase reporter assay. **C.** VEGFB mRNA levels within OC tissues were measured by RT-qPCR. **D.** Correlation of VEGFB expression with miR-133a-5p within OSCC tissue samples was measured via Spearman correlation. **E-F.** VEGFB mRNA and protein levels within OSCC cells following miR-133a-5p mimic transfection were analyzed through RT-qPCR and WB assays. Results are means from 3 individual assays. *P<0.05, **P<0.01, ***P<0.001.

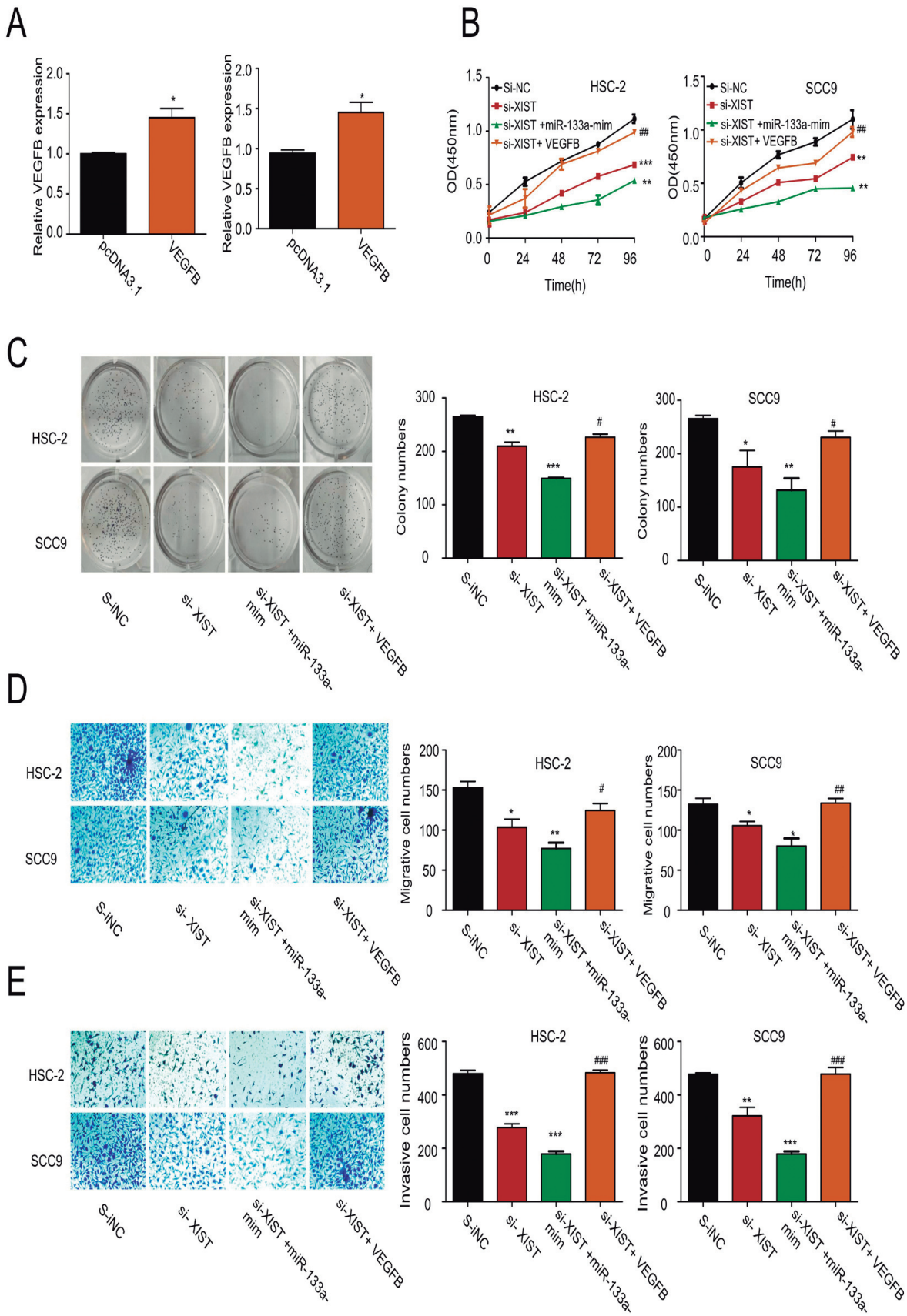

Fig 6. XIST promotes OSCC malignant behavior through modulating miR-133a-5p/VEGFB axis. si-NC (siRNA negative control), si-XIST (XIST siRNA), si-XIST +miR-133a-5p mimic or si-XIST+ VEGFB (VEGFB expression vector) were transfected into HSC-2 and SCC9 cells. **A.** VEGFB mRNA level after transfecting with VEGFB expression construct was evaluated by qRT-PCR. **B.** CCK-8 assay was conducted to determine cell proliferation at 0/24/48/72/96h following the indicated treatment. **C.** Clonogenic capacity was determined by clone forming assay. Transwell assays were conducted to determine cell migration **(D)** and **(E)** invasion in HSC-2 and SCC9 cells after the indicated treatment. *P<0.05, **P<0.01, ***P<0.001; # indicates statistical comparison of si-XIST with si-XIST+VEGFB groups.

luciferase reporter assay using WT or MUT reporter containing VEGFB mRNA 3' UTR, miR-133a-5p mimic remarkably suppressed the luciferase activity of WT-VEGFB reporter, while the activity of MUT-VEGFB reporter was not affected (Fig. 5B). Moreover, VEGFB mRNA level was significantly elevated in OSCC samples relative to non-carcinoma normal samples (Fig. 5 C). As suggested by Spearman correlation, miR-133a-5p level was negatively correlated with VEGFB level in OSCC tissues (Fig. 5D). Both VEGFB protein and mRNA levels were significantly downregulated upon the transfection of miR-133a-5p mimic (Fig. 5D,E). Together, based on the above results, VEGFB serves as a downstream target of miR-133a-5p, which is under negative control by miR-133a-5p.

XIST regulates the malignancy of OSCC cells through modulating the miR-133a-5p/VEGFB axis

To explore the biological interactions between the miR-133a-5p/VEGFB axis and XIST in OSCC cells, we transfected HSC-2 and SCC9 cells with si-NC, si-XIST si-XIST+miR-133a-5p mimic, or si-XIST+VEGFB (VEGFB expression vector). Cells under the above conditions were subject to cell growth, invasion and migration assays. The VEGFB overexpression upon the transfection of VEGFB expression vector was confirmed by RT-qPCR (Fig. 6A). Interestingly, both colony formation and CCK-8 proliferation assays revealed that VEGFB overexpression abolished the inhibitory effects of XIST silencing on cell proliferation (Fig. 6B,C). In addition, transwell assay also demonstrated that VEGFB overexpression enhanced cell invasion and migration capacities upon XIST silencing (Fig. 6D,E). Collectively, these data suggest that XIST regulates OSCC malignant features by targeting the miR-133a-5p/VEGFB axis.

Discussion

As discovered in this work, lncRNA XIST expression was remarkably elevated in OSCC samples and OSCC cells, while XIST silencing inhibited the growth, invasion and migration of OSCC cells. LncRNAs can modulate gene levels epigenetically, transcriptionally, and post-transcriptionally, which are related to various cellular processes such as proliferation, metabolism, migration, apoptosis and differentiation (Ye et al., 2014). LncRNA XIST was upregulated in different forms of cancers, and the elevated XIST level was proposed to be a prognostic biomarker (Hu et al., 2018). For example, XIST accounts for the possible oncogenic factor significantly upregulated within both colorectal cancer (CRC) cells and tissues, and the upregulation of XIST enhanced CRC cell growth by suppressing miR-132-3p (Song et al., 2017). XIST overexpression remarkably promotes pancreatic cancer cell growth, invasion and migration, but suppresses their apoptosis (Sun et al., 2018). In addition, upregulated lncRNA XIST has been demonstrated to contribute to the progression of cervical cancer and ovarian cancer (Chen et al., 2019; Jiang et al., 2021). A recent study further showed that XIST is involved in OSCC development by sponging miR-455-3p (Li et al., 2020b). Our study also suggests that XIST upregulation predicts a poorer overall survival, a relatively greater tumor size and later tumor stage among OSCC cases. Therefore, the previous reports of XIST upregulation in various cancers and our finding in OSCC support the oncogenic function of XIST in different cancers.

Our study also revealed that silencing XIST results in impaired OSCC cell invasion and migration. An extracellular matrix (ECM) protein such as osteopontin is related to tumor development, cell invasion and migration (Rodrigues et al., 2007). Interestingly, XIST was reported to regulate osteopontin level through targeting miR-376c-5p in macrophages (Li et al., 2020a), while the XIST/miR-9-5p/ALPL (Alkaline Phosphatase) axis can also regulate the expression of osteopontin within human bone marrow mesenchymal stem cells (BMSCs) (Zheng et al., 2020a). Future efforts are required to determine whether XIST also regulates the ECM component levels in OSCC cells to modulate invasion and migration. Our data further showed that silencing XIST downregulates the expression of mesenchymal markers in OSCC cells. Consistently, XIST upregulation expedites metastasis and modulates epithelial-mesenchymal transition (EMT) in colorectal cancer (Chen et al., 2017). Suppressing XIST expression is able to inhibit cell migration and EMT in non-small cell lung cancer cells (Qiu et al., 2019). Therefore, XIST upregulation can contribute to the progression of different cancers via promoting EMT and cell migration.

miR-133a-5p was identified as XIST's potential target, and their functional interaction was validated by dual luciferase reporter sassy. Over 2675 miRNAs have been identified in human cells, and an estimated 30% of human genes are regulated by miRNAs (Calin et al., 2004; Garzon et al., 2006). miRNAs regulate diverse biological processes, including cell cycle, cell proliferation, energy metabolism, stress tolerance, energy metabolism and apoptosis. (Calin et al., 2004; Garzon et al., 2006) miRNAs can act as both oncogenic factors and tumor suppressors in different tumors. In the meanwhile, lncRNAs can serve as competitive endogenous RNAs to interfere with the binding of miRNAs to their targets (Hirata et al., 2015). Based on our results, miR-133a-5p is a tumor suppressor in OSCC, which is negatively regulated by XIST. Similarly, prior works reported that miR133a can act as tumor suppressor in different cancers. For instance, miR133a induced apoptosis by regulating glutathione Stransferase pi 1 (GSTP1) in bladder cancer cell lines (Uchida et al., 2013), and inhibited bladder cancer cell growth, migration and metastasis through targeting epidermal growth factor receptor (EGFR) (Zhou et al., 2019). miR-133a also attenuated malignant features of

osteosarcoma, lung cancer and glioma cells (Xu and Wang, 2013; Chen et al., 2016; Sakr et al., 2016). In a recent study on OSCC, miR-133a-5p regulated tumor progression through targeting Paired Related Homeobox 1 (PRX1) (Zhang et al., 2021). However, the tumor suppressive effect of miR-133a-5p in OSCC needs to be further evaluated in animal models.

VEGFB is one of the best-studied genes of the VEGF family. Yang et al. reported that VEGFB was differentially expressed in different tumor cell lines such as ovarian cancer, breast cancer (BC), melanoma and renal cell carcinoma (RCC), with UACC-257 melanoma cell line expressing the highest level (Yang et al., 2015). VEGFB enhances the metastasis of tumor cells and has been recognized as an unfavorable prognostic biomarker in cancer patients (Yang et al., 2015). Consistent with these observations, we showed that VEGFB expression was upregulated in OSCC samples, which showed a negative correlation with miR-133a-5p. Since the overexpression of VEGFB can rescue the inhibitory effects of XIST silencing on cell growth, invasion and migration, our study indicates that VEGFB functions as a downstream effector, mediating the oncogenic effect of XIST. This is because XIST negatively regulates miR-133a-5p and miR-133a-5p negatively regulates VEGFB expression. Silencing XIST would lead to the upregulation of miR-133a-5p and the downregulation of VEGFB, and VEGFB overexpression replenishes VEGFB level to abolish the silencing effect of XIST on VEGFB expression and the inhibitory effects of XIST silencing on cell phenotype. Future study is required to clarify whether the XIST/miRNA/VEGFB axis is also implicated in other types of cancers.

It is worth mentioning that Human Papillomavirus (HPV), a prevalent human viral infection and the causal agent of cervical cancer, appears to be involved in the etiology of oral cancer (Herrero et al., 2003). A previous study suggested acid sphingomyelinase activity as an indicator of cell stress in HPV-positive and HPV-negative head and neck squamous cell carcinoma (Gerle et al., 2018). It remains to be determined whether the HPV status regulates the expression of XIST and the malignant phenotype in OSCC.

Conclusions

The current study showed that both XIST and VEGFB level were significantly elevated in OSCC tissues, whereas miR-133a-5p expression was decreased. Moreover, our data further demonstrated that XIST seems to act as an oncogenic factor to promote the growth, migration and invasion of OSCC cells via modulating the miR-133a-5p/VEGFB axis. Those data suggest that XIST/miR-133a/VEGFB axis might serve as potential anti-OSCC therapeutic targets. Future works are required to validate the functional engagement of the XIST/miR-133a/VEGFB axis in the tumorigenesis of OSCC in animal models.

Funding. This work is supported by the 2021 Guangdong Provincial Medical Research Fund (No. A2021495).

Competing interests. All authors declare no competing interests.

References

Blot W.J., McLaughlin J.K., Winn D.M., Austin D.F., Greenberg R.S., Preston-Martin S., Bernstein L., Schoenberg J.B., Stemhagen A. and Fraumeni J.F. Jr. (1988). Smoking and drinking in relation to oral and pharyngeal cancer. Cancer Res. 48, 3282-3287.

Bray F., Ferlay J., Soerjomataram I., Siegel R.L., Torre L.A. and Jemal A. (2018). Global cancer statistics 2018: GLOBOCAN estimates of incidence and mortality worldwide for 36 cancers in 185 countries. CA Cancer J. Clin. 68, 394-424.

Calin G.A., Sevignani C., Dumitru C.D., Hyslop T., Noch E., Yendamuri S., Shimizu M., Rattan S., Bullrich F., Negrini M. and Croce C.M. (2004). Human microRNA genes are frequently located at fragile sites and genomic regions involved in cancers. Proc. Natl. Acad. Sci. USA 101, 2999-3004.

Cerase A., Pintacuda G., Tattermusch A. and Avner P. (2015). Xist localization and function: new insights from multiple levels. Genome Biol. 16, 166.

Chen G., Fang T., Huang Z., Qi Y., Du S., Di T., Lei Z., Zhang X. and Yan W. (2016). MicroRNA-133a inhibits osteosarcoma cells proliferation and invasion via targeting IGF-1R. Cell Physiol. Biochem. 38, 598-608.

Chen D.L., Chen L.Z., Lu Y.X., Zhang D.S., Zeng Z.L., Pan Z.Z., Huang P., Wang F.H., Li Y.H., Ju H.Q. and Xu R.H. (2017). Long noncoding RNA XIST expedites metastasis and modulates epithelial-mesenchymal transition in colorectal cancer. Cell Death Dis. 8, e3011.

Chen X., Xiong D., Ye L., Wang K., Huang L., Mei S., Wu J., Chen S., Lai X., Zheng L. and Wang M. (2019). Up-regulated lncRNA XIST contributes to progression of cervical cancer via regulating miR-140-5p and ORC1. Cancer Cell Int. 19, 45.

Cheng Z., Liu F., Wang G., Li Y., Zhang H. and Li F. (2014). miR-133 is a key negative regulator of CDC42-PAK pathway in gastric cancer. Cell Signal 26, 2667-2673.

Esteller M. (2011). Non-coding RNAs in human disease. Nat. Rev. Genet. 12, 861-874.

Ferlay J., Shin H.R., Bray F., Forman D., Mathers C. and Parkin D.M. (2010). Estimates of worldwide burden of cancer in 2008: GLOBOCAN 2008. Int. J. Cancer 127, 2893-2917.

Figuero Ruiz E., Carretero Peláez M.A., Cerero Lapiedra R., Esparza Gómez G. and Moreno López L.A. (2004). Effects of the consumption of alcohol in the oral cavity: relationship with oral cancer. Med. Oral 9, 14-23.

Garzon R., Fabbri M., Cimmino A., Calin G.A. and Croce C.M. (2006). MicroRNA expression and function in cancer. Trends. Mol. Med. 12, 580-587.

Gerle M., Medina T.P., Gülses A., Chu H., Naujokat H., Wiltfang J. and Açil Y. (2018). Acid sphingomyelinase activity as an indicator of the cell stress in HPV-positive and HPV-negative head and neck squamous cell carcinoma. Med. Oncol. 35, 58.

Guo Y., Sun P., Guo W. and Dong Z. (2021). Long non-coding RNA LINC01503 promotes gastric cardia adenocarcinoma progression

via miR-133a-5p/VIM axis and EMT process. Dig. Dis. Sci. 66, 3391-3403.

Herrero R., Castellsagué X., Pawlita M., Lissowska J., Kee F., Balaram P., Rajkumar T., Sridhar H., Rose B., Pintos J., Fernández L., Idris A., Sánchez M.J., Nieto A., Talamini R., Tavani A., Bosch F.X., Reidel U., Snijders P.J., Meijer C.J., Viscidi R., Muñoz N. and Franceschi S. (2003). Human papillomavirus and oral cancer: the International Agency for Research on Cancer multicenter study. J. Natl. Cancer Inst. 95, 1772-1783.

Hirata H., Hinoda Y., Shahryari V., Deng G., Nakajima K., Tabatabai Z.L., Ishii N. and Dahiya R. (2015). Long noncoding RNA MALAT1 promotes aggressive renal cell carcinoma through Ezh2 and Interacts with miR-205. Cancer Res. 75, 1322-1331.

Hu Y., Deng C., Zhang H., Zhang J., Peng B. and Hu C. (2017). Long non-coding RNA XIST promotes cell growth and metastasis through regulating miR-139-5p mediated Wnt/β-catenin signaling pathway in bladder cancer. Oncotarget 8, 94554-94568.

Hu S., Chang J., Li Y., Wang W., Guo M., Zou E.C., Wang Y. and Yang Y. (2018). Long non-coding RNA XIST as a potential prognostic biomarker in human cancers: a meta-analysis. Oncotarget 9, 13911-13919.

Hu B., Shi G., Li Q., Li W. and Zhou H. (2019). Long noncoding RNA XIST participates in bladder cancer by downregulating p53 via binding to TET1. J. Cell Biochem. 120, 6330-6338.

Jiang R., Zhang H., Zhou J., Wang J., Xu Y., Zhang H., Gu Y., Fu F., Shen Y., Zhang G., Feng L., Zhang X., Chen Y. and Shen F. (2021). Inhibition of long non-coding RNA XIST upregulates microRNA-149-3p to repress ovarian cancer cell progression. Cell Death Dis. 12, 145.

Jin H., Li D., Wang X., Jia J., Chen Y., Yao Y., Zhao C., Lu X., Zhang S., Togo J., Ji Y., Zhang L., Feng X. and Zheng Y. (2018). VEGF and VEGFB play balancing roles in adipose differentiation, gene expression, and function. Endocrinology 159, 2036-2049.

Kim S.K., Park S.G. and Kim K.W. (2015). Expression of vascular endothelial growth factor in oral squamous cell carcinoma. J. Korean Assoc. Oral Maxillofac. Surg. 41, 11-18.

Kondo Y., Shinjo K. and Katsushima K. (2017). Long non-coding RNAs as an epigenetic regulator in human cancers. Cancer Sci. 108, 1927-1933.

Lal N., Chiu A.P., Wang F., Zhang D., Jia J., Wan A., Vlodavsky I., Hussein B. and Rodrigues B. (2017). Loss of VEGFB and its signaling in the diabetic heart is associated with increased cell death signaling. Am. J. Physiol. Heart Circ. Physiol. 312, H1163-h1175.

Li L., Lv G., Wang B. and Kuang L. (2020a). XIST/miR-376c-5p/OPN axis modulates the influence of proinflammatory M1 macrophages on osteoarthritis chondrocyte apoptosis. J. Cell Physiol. 235, 281-293.

Li Q., Sun Q. and Zhu B. (2020b). LncRNA XIST inhibits the progression of oral squamous cell carcinoma via sponging miR-455-3p/BTG2 axis. Onco. Targets Ther. 13, 11211-11220.

Liu J., Yao L., Zhang M., Jiang J., Yang M. and Wang Y. (2019a). Downregulation of LncRNA-XIST inhibited development of non-small cell lung cancer by activating miR-335/SOD2/ROS signal pathway mediated pyroptotic cell death. Aging (Albany NY) 11, 7830-7846.

Liu S., Chen J., Zhang T. and Chen H. (2019b). MicroRNA-133 inhibits the growth and metastasis of the human lung cancer cells by targeting epidermal growth factor receptor. J.BUON 24, 929-935.

Lv G.Y., Miao J. and Zhang X.L. (2018). Long noncoding RNA XIST promotes osteosarcoma progression by targeting Ras-related protein RAP2B via miR-320b. Oncol. Res. 26, 837-846.

Ma L., Zhou Y., Luo X., Gao H., Deng X. and Jiang Y. (2017). Long non-coding RNA XIST promotes cell growth and invasion through regulating miR-497/MACC1 axis in gastric cancer. Oncotarget 8, 4125-4135.

Mercer T.R., Dinger M.E. and Mattick J.S. (2009). Long non-coding RNAs: insights into functions. Nat. Rev. Genet. 10, 155-159.

Petti S., Masood M., Messano G.A. and Scully C. (2013). Alcohol is not a risk factor for oral cancer in nonsmoking, betel quid non-chewing individuals. A meta-analysis update. Ann. Ig. 25, 3-14.

Qiu H.B., Yang K., Yu H.Y. and Liu M. (2019). Downregulation of long non-coding RNA XIST inhibits cell proliferation, migration, invasion and EMT by regulating miR-212-3p/CBLL1 axis in non-small cell lung cancer cells. Eur. Rev. Med. Pharmacol. Sci. 23, 8391-8402.

Rodrigues L.R., Teixeira J.A., Schmitt F.L., Paulsson M. and Lindmark-Mänsson H. (2007). The role of osteopontin in tumor progression and metastasis in breast cancer. Cancer Epidemiol. Biomarkers Prev. 16, 1087-1097.

Sakr M., Takino T., Sabit H., Nakada M., Li Z. and Sato H. (2016). miR-150-5p and miR-133a suppress glioma cell proliferation and migration through targeting membrane-type-1 matrix metalloproteinase. Gene 587, 155-162.

Song H., He P., Shao T., Li Y., Li J. and Zhang Y. (2017). Long non-coding RNA XIST functions as an oncogene in human colorectal cancer by targeting miR-132-3p. J. BUON 22, 696-703.

Sun Z., Zhang B. and Cui T. (2018). Long non-coding RNA XIST exerts oncogenic functions in pancreatic cancer via miR-34a-5p. Oncol. Rep. 39, 1591-1600.

Tao J., Wu D., Xu B., Qian W., Li P., Lu Q., Yin C. and Zhang W. (2012). microRNA-133 inhibits cell proliferation, migration and invasion in prostate cancer cells by targeting the epidermal growth factor receptor. Oncol. Rep. 27, 1967-1975.

Uchida Y., Chiyomaru T., Enokida H., Kawakami K., Tatarano S., Kawahara K., Nishiyama K., Seki N. and Nakagawa M. (2013). MiR-133a induces apoptosis through direct regulation of GSTP1 in bladder cancer cell lines. Urol. Oncol. 31, 115-123.

Vennin C., Spruyt N., Dahmani F., Julien S., Bertucci F., Finetti P., Chassat T., Bourette R.P., Le Bourhis X. and Adriaenssens E. (2015). H19 non coding RNA-derived miR-675 enhances tumorigenesis and metastasis of breast cancer cells by downregulating c-Cbl and Cbl-b. Oncotarget 6, 29209-29223.

Vitt U.A., Hsu S.Y. and Hsueh A.J. (2001). Evolution and classification of cystine knot-containing hormones and related extracellular signaling molecules. Mol. Endocrinol. 15, 681-694.

Wang T., Wang X., Du Q., Wu N., Liu X., Chen Y., and Wang X. (2019). The circRNA circP4HB promotes NSCLC aggressiveness and metastasis by sponging miR-133a-5p. Biochem. Biophys. Res. Commun. 513, 904-911.

Xia H. and Hui K.M. (2014). Mechanism of cancer drug resistance and the involvement of noncoding RNAs. Curr. Med. Chem. 21, 3029-3041.

Xu M. and Wang Y.Z. (2013). miR-133a suppresses cell proliferation, migration and invasion in human lung cancer by targeting MMP-14. Oncol. Rep. 30, 1398-1404.

Yang X., Zhang Y., Hosaka K., Andersson P., Wang J., Tholander F., Cao Z., Morikawa H., Tegnér J., Yang Y., Iwamoto H., Lim S. and Cao Y. (2015). VEGF-B promotes cancer metastasis through a VEGF-A-independent mechanism and serves as a marker of poor prognosis for cancer patients. Proc. Natl. Acad. Sci. USA 112, E2900-2909.

Ye Z.Q., Wang T. and Song W. (2014). Long noncoding RNAs in prostate cancer. Zhonghua Nan Ke Xue 20, 963-968 (in Chinese).

Yin L., Chen J., Ma C., Pei S., Du M., Zhang Y., Feng Y., Yin R., Bian X., He X. and Feng J. (2020). Hsa_circ_0046263 functions as a ceRNA to promote nasopharyngeal carcinoma progression by upregulating IGFBP3. Cell Death Dis. 11, 562.

Zhang X.T., Pan S.X., Wang A.H., Kong Q.Y., Jiang K.T. and Yu Z.B. (2019). Long non-coding RNA (lncRNA) X-inactive specific transcript (XIST) plays a critical role in predicting clinical prognosis and progression of colorectal cancer. Med. Sci. Monit. 25, 6429-6435.

Zhang N., Zeng L., Wang S., Wang R., Yang R., Jin Z. and Tao H. (2021). LncRNA FER1L4 promotes oral squamous cell carcinoma progression via targeting miR-133a-5p/Prx1 axis. Onco. Targets Ther. 14, 795-806.

Zheng C., Bai C., Sun Q., Zhang F., Yu Q., Zhao X., Kang S., Li J. and Jia Y. (2020a). Long noncoding RNA XIST regulates osteogenic differentiation of human bone marrow mesenchymal stem cells by targeting miR-9-5p. Mech. Dev. 162, 103612.

Zheng L., Kang Y., Zhang L. and Zou W. (2020b). MiR-133a-5p inhibits androgen receptor (AR)-induced proliferation in prostate cancer cells via targeting FUsed in Sarcoma (FUS) and AR. Cancer Biol. Ther. 21, 34-42.

Zhou Y., Wu D., Tao J., Qu P., Zhou Z. and Hou J. (2013). MicroRNA-133 inhibits cell proliferation, migration and invasion by targeting epidermal growth factor receptor and its downstream effector proteins in bladder cancer. Scand. J. Urol. 47, 423-432.

Zhou K., Yang J., Li X. and Chen W. (2019). Long non-coding RNA XIST promotes cell proliferation and migration through targeting miR-133a in bladder cancer. Exp. Ther. Med. 18, 3475-3483.

Zhu H., Zheng T., Yu J., Zhou L. and Wang L. (2018). LncRNA XIST accelerates cervical cancer progression via upregulating Fus through competitively binding with miR-200a. Biomed. Pharmacother. 105, 789-797.

Accepted August 1, 2022